J. Hydrau., Coast. Environ. Eng., JSCE, No. 614/II-46, 121-133, 1999 February

NUMERICAL MODELLING OF NONLINEAR INTERACTION BETWEEN WAVE AND COMPOSITE BREAKWATER OVER SAND SEABED

Norimi MIZUTANI[1], Ayman M. MOSTAFA[2] and Koichiro IWATA[3]

[1] Member of JSCE, Dr. of Eng., Assoc. Prof., Dept. of Civil Eng., Nagoya Univ. (Nagoya 464-8603, Japan)
[2] Member of JSCE, Dr. of Eng., Res. Assoc., Dept. of Civil Eng., Nagoya Univ. (Nagoya 464-8603, Japan)
[3] Member of JSCE, Dr. of Eng., Prof., Dept. of Civil Eng., Nagoya Univ. (Nagoya 464-8603, Japan)

Experiments were conducted to verify the validity of the BEM-FEM and poro-elastic FEM models, developed by the authors, for composite breakwaters. The BEM-FEM model is confirmed to predict well the wave field. The poro-elastic FEM model uses an equivalent nonlinear Darcy coefficient of permeability and runs under the surface pressure computed by the BEM-FEM model. The poro-elastic model computes the pore pressure in the porous media more accurately than the BEM-FEM model. The transmitted wave characteristics along with the dynamic behaviour of the composite breakwater and seabed are investigated. A study is conducted to find out the parameters causing a high pressure gradient at the offshore toe.

Key Words: *nonlinear waves, sand seabed, composite breakwaters, poro-elastic models, wave-structure-foundation dynamic interaction*

1. GENERAL

Composite breakwater is the most common type of breakwaters constructed in Japan to produce a calm sea in the harbour area. The composite breakwater usually has a vertical face caisson installed on a rubble base. The wave force mainly acts on the caisson but still induces stresses in the rubble base and seabed. Early research focused on the wave forces acting on the caisson with less interest to the dynamic interaction between the caisson, rubble base and seabed. Static methods have also been used to compute the stresses in the rubble base and seabed due to the wave force acting on the caisson.

Oumeraci[1] classified the failure modes of a vertical breakwater into local and overall failure modes. He also reported the occurrence of scour in the seabed near the offshore toe and the possibility of punching failure under the caisson edges. Oumeraci and Kortenhaus[2] also examined the dynamic response of a caisson breakwater subject to breaking waves. They introduced a quasi-static linear numerical model which considers only the horizontal and rotational motion of the caisson. The dynamic interaction between the caisson and soil foundation was further treated only through an added mass term in the equations of caisson motion. Kortenhaus et al.[3] studied the wave-induced uplift of caisson breakwater and confirmed the existence of small waves behind the caisson using a large scale model.

The linear wave field around composite breakwaters and the stability of its rubble base were studied while disregarding the seabed[4]. The linear wave theory in the wave domain and the linearized porous flow equations were adopted to facilitate the use of the BEM inside and outside the porous media.

Other researchers[5], [6] considered the rubble base as a rigid impermeable medium which acts only to transmit the caisson stresses to the seabed. They developed an analytical solution for the caisson-induced stresses in the seabed and compared it with a physical model and a numerical model. Mase et al.[7] developed a poro-elastic FEM model for composite breakwaters subject to linear waves on the offshore side only.

Mizutani et al.[8] compared the resistance coefficients in Navier-Stokes equations for flow in porous media, developed by McCorquodale et al.[9], with those in Morison-type equations. They revised the coefficients in the porous flow equations and developed a BEM-FEM model to study the nonlinear interaction between wave and submerged breakwater.

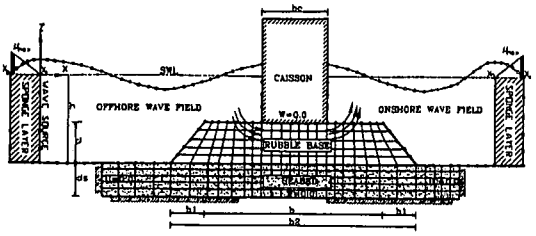

Fig.1 Problem definition and layout of nodes

Mostafa and Mizutani[10] improved the BEM-FEM model and included the seabed in the solution domain. They developed a poro-elastic FEM model to study the dynamic interaction between a structure and its seabed foundation. The latter model runs for the surface pressure computed by the BEM-FEM model. They first applied these models to a seawall over a sand seabed subject to nonlinear waves. The models were adapted to study a hydraulic model of submerged breakwater over a sand seabed and the models' validity was confirmed[11]. Further verification was made for the case of composite breakwater model over a sand bottom[12]. However, the effects of various wave, structure and site conditions have not been discussed yet. Instability problems were reported on the offshore toe of a rubble base[1] and, hence, investigating this location helps to explain the mechanism of such problems.

2. SCOPE OF WORK

This work covers further details on the nonlinear interaction among wave, composite breakwater and seabed including the effects of various wave, structure and site conditions. The technique for computing a nonlinear Darcy permeability in the poro-elastic FEM model is first presented and the numerical results are compared with those of the BEM-FEM model. Experimental results are used to examine the validity of the numerical models. The effect of the internal properties of the rubble base and the incident wave conditions on the characteristics of the nonlinear reflected and transmitted waves is uniquely illuminated here. The dynamic behaviour of a composite breakwater is analyzed for different thickness and shear modulus of the seabed as well as various stiffness of the rubble base. The factors affecting the pore pressure at the offshore toe are also investigated.

3. NUMERICAL MODELS

(1) BEM-FEM Model

In the wave field, the fluid is considered to be inviscid and incompressible and its motion is irrotational and governed by the following Poisson-type equation:

$$\frac{\partial^2\phi}{\partial X^2}+\frac{\partial^2\phi}{\partial Z'^2}=q \tag{1}$$

where ϕ is the velocity potential; X and Z′ are the horizontal and vertical coordinates, respectively; and q is the flux density at the wave source and is zero elsewhere.

The wave tank has onshore and offshore wave fields. The open boundaries are closed by the sponge layers developed in the idealized wave tank of Ohyama and Nadaoka[13]. The incident wave is generated by a non-refelective wave source[14]. The transmitted wave is caused mainly by the wave passing through the pores of the rubble base.

The pore fluid is considered to be incompressible but viscous and its flow may be rotational. The fluid in the porous media is governed by the continuity and modified Navier-Stokes equations of motion[8].

$$\frac{\partial U}{\partial X}+\frac{\partial W}{\partial Z'}=0 \tag{2}$$

$$A\frac{\partial U}{\partial t}+BU\frac{\partial U}{\partial X}+BW\frac{\partial U}{\partial Z'}+C\frac{\partial P}{\partial X}+EU+FUV=0 \tag{3}$$

$$A\frac{\partial W}{\partial t}+BU\frac{\partial W}{\partial X}+BW\frac{\partial W}{\partial Z'}+C\frac{\partial P}{\partial Z'}+EW+FWV=0 \tag{4}$$

and

$$A=\frac{1+\frac{1-m}{m}C_a}{mg}$$

$$B=\frac{1}{m^2g}$$

$$C=\frac{1}{\gamma}$$

$$E=\frac{6(1-m)\upsilon C_{D2}}{gm^2D^2}$$

$$F=\frac{C_{D1}(1-m)}{2gm^3D}$$

$$P=p-\gamma Z'$$

where U, W and V are the horizontal, vertical and total seepage velocities, respectively; P and p are the total and dynamic pore pressure, respectively; m is the porosity; g is the acceleration of gravity; C_a is the coefficient of added mass; γ is the unit weight of water; υ is the kinematic viscosity; D is the mean diameter of solids; and C_{D1} and C_{D2} are the coefficients of drag defined in Mizutani et al.[8].

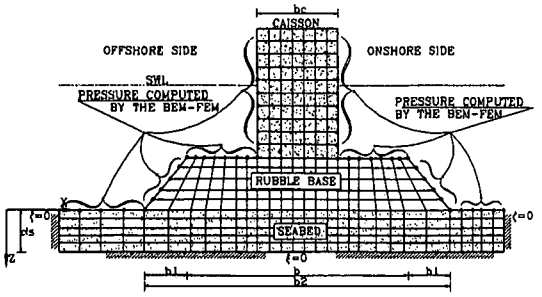

Fig.2 Layout of nodes for the poro-elastic model

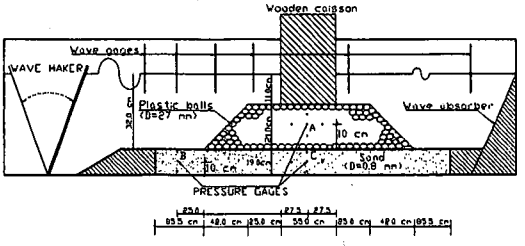

Fig.3 2-D wave tank experiment

The BEM was applied to the wave field and the FEM was utilized to solve the porous flow field. The continuity of the normal velocity component and the pressure at the separating boundary was considered. The *cold start* was adopted as an initial condition and the computations progress in a time marching scheme till the requested time step. Details about this technique are found in Mostafa and Mizutani[10].

(2) Poro-Elastic FEM Model

The poro-elastic model adopts Biot's equations[15] which consider the pore flow to obey Darcy's law and the solids' deformation to follow Hooke's law. The pore fluid is assumed to be a single compressible phase that is composed of water and tinny gas bubbles. Thus, the governing equations read:

$$G\nabla^2\zeta + \frac{G}{1-2\nu}\frac{\partial\varepsilon}{\partial X} = \frac{\partial p}{\partial X} \quad (5)$$

$$G\nabla^2\xi + \frac{G}{1-2\nu}\frac{\partial\varepsilon}{\partial Z} = \frac{\partial p}{\partial Z} \quad (6)$$

$$\frac{K}{\gamma}\nabla^2 p = \frac{m}{\beta}\frac{\partial p}{\partial t} + \frac{\partial\varepsilon}{\partial t} \quad (7)$$

$$\varepsilon = \frac{\partial\zeta}{\partial X} + \frac{\partial\xi}{\partial Z} \quad (8)$$

where G is the shear modulus of the medium; ζ and ξ are the horizontal and vertical solid displacements, respectively; Z is the vertical axis defined by **Fig.2**; ν is Poisson's ratio; K is the coefficient of permeability; and β is the bulk modulus of pore fluid.

The FEM was employed to solve the poro-elastic equations and the model is called poro-elastic FEM model. The caisson, rubble base and seabed were treated as poro-elastic media to maintain their mutual dynamic interaction due to the wave pressure computed by the BEM-FEM at each time step in a time-marching scheme. The *cold start* was also utilized as an initial condition. Details of the model were explained in Mostafa and Mizutani[10].

4. HYDRAULIC MODEL

A composite breakwater model was constructed in the two-dimensional wave tank of Nagoya University. A wooden caisson model was placed over a perforated steel cage, filled with plastic and glass balls, laid on a sand seabed. Dimensions and properties of the breakwater and seabed are shown in **Fig.3**. Waves of 1.4, 1.8 and 2.2s period (T) and of 3.0, 5.0 and 7.0cm incident height (H) were tested. Wave breaks in case of H=7.0 cm and does not for smaller heights.

The water levels, on both sides of the breakwater, and the pore pressure (at "A", "B" and "C") were recorded from the still water condition at a sampling time of 0.02s for about 15 waves. Five pressure gages were arranged in a cross-shape-like layout and fixed to a thin frame. The pore pressure at every location was measured twice. Even if, the differences between both records are minor, the average has been adopted for comparison with the numerical models.

5. COMPARISON OF MODELS

The hydraulic conductivity in the modified Navier-Stokes equations of motion is represented in terms of the porosity; the mean size of the solids; and the drag and inertia coefficients. It can be readily noticed that, by neglecting the convective acceleration terms, the nonlinear Darcy coefficient of permeability (K_n) for steady flow can be expressed as follows:

$$K_n = \frac{1}{E + FV} \quad (9)$$

The term "E" represents the linear Darcy coefficient of permeability and its value has minor effect on K_n when the effect of "FV" dominates; e.g., in the rubble base. However, at low values of V, the value of K_n is nearly 1/E; e.g., in the sand seabed.

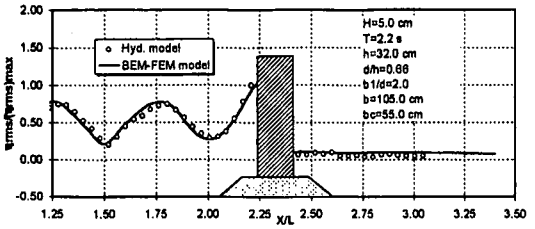

Fig.4 Computed and measured η_{rms} values (H/h=0.16 & h/gT^2=0.007)

To compare the results of the BEM-FEM and poro-elastic FEM models, taking into account that Biot's equations are derived for a linear Darcy permeability, the value of K is computed by Eq.9, i.e., $K=K_n$, and considering $V=\Sigma V_{max}/N$; where N is the number of nodes. Thus, K≅0.22cm/s for the sand seabed (D=0.08cm, m=0.30, υ=0.01cm^2/s, C_{D2}=60 and C_{D1}=0.35) and K≅16.0cm/s for the rubble base (D=2.70cm, m=0.24, υ=0.01cm^2/s, C_{D2}=25, C_{D1}=0.45, H=5.0cm and T=2.2s) were used. The estimated permeability of the seabed is close to that by Ergun[16] and that in the rubble base is also comparable to that by Dudgeon[17]. The shear modulus of the rubble base and the seabed is assumed to be 10^{10} and $5x10^9$Dyn/cm^2, respectively. A value of $\beta=5x10^7$Dyn/cm^2 is employed in the computations corresponding to 98% pore fluid saturation as in Yamamoto et al.[18].

The value of η_{rms} along the wave tank is correlated to the wave energy and may represent it. Comparison is made between the measured and computed values of η_{rms} for H=5.0cm and T=2.2s. **Fig.4** shows that the BEM-FEM predicts fairly well the experimental results. The instantaneous water levels are compared at location "B" of the pressure gages, i.e., X/L≅2.0, where L is the incident wave length. **Fig.5a** confirms the ability of the BEM-FEM model to predict the instantaneous water levels. A secondary crest is also evident at location "B".

The measured pore pressure, by the gages at the mid-height of the pressure gages' frame, is compared with that computed by the numerical models in **Fig.5b-d** and good agreement can be seen. The poro-elastic model has a better accuracy than the BEM-FEM model to evaluate the pore pressure in the seabed. It is also observed that the dissipation of higher harmonics in the seabed is obvious in the poro-elastic and hydraulic models but it is less obvious in the BEM-FEM model. This causes the differences in the pore pressure magnitude between the hydraulic and BEM-FEM models to become larger at points far below the seabed level (**Fig.5e**).

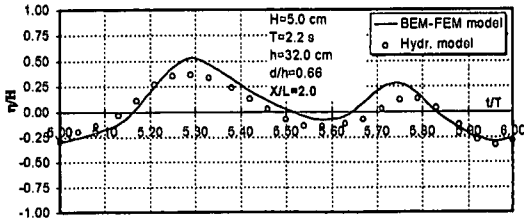

Fig.5a Water levels over "B" (X/L=2.0)

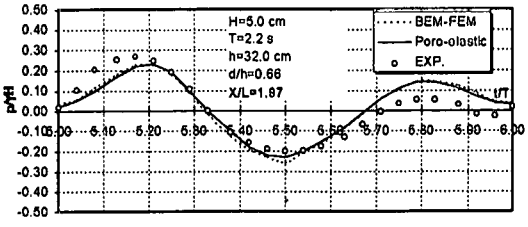

Fig.5b Pore pressure at "B" (X/L=1.97)

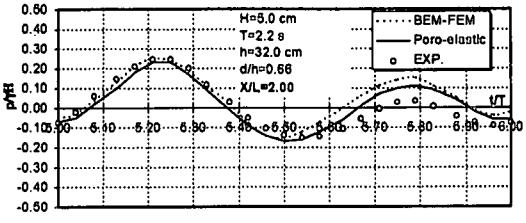

Fig.5c Pore pressure at "B" (X/L=2.0)

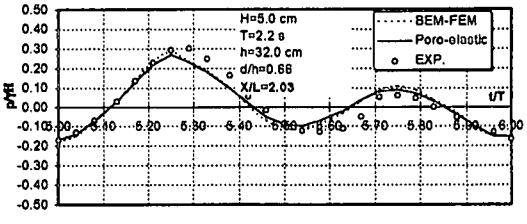

Fig.5d Pore pressure at "B" (X/L=2.03)

The pore pressure in the rubble base seems to include higher harmonics whose amplitudes are damped with a phase shift towards the onshore side (**Fig.6a-b**). The computed pore pressure in the rubble base agrees reasonably with the hydraulic model, but the BEM-FEM model results show a better agreement. This may be because the poro-elastic model approximates the flow in the rubble base by an equivalent linear Darcy coefficient while the BEM-FEM employs a nonlinear one. The differences observed in the results suggest the development of a nonlinear flow poro-elastic model for the simulation of porous flow in coarse granular materials. Other details and proofs for the validity of the numerical models are found in Mizutani and Mostafa[19] and Mostafa et al.[12].

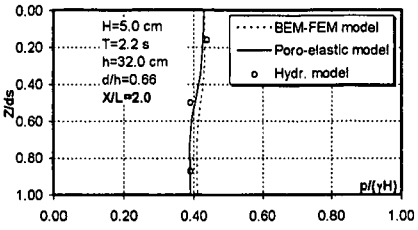

Fig.5e Pore pressure magnitude at "B" (X/L=2.0)

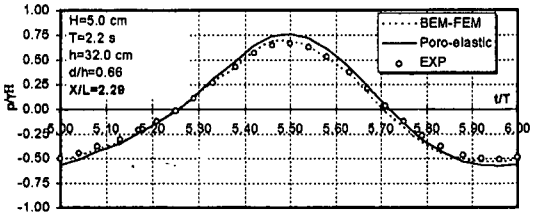

Fig.6a Pore pressure at "A" (X/L=2.29 & Z'/h=-0.69)

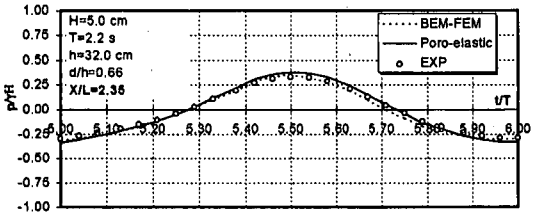

Fig.6b Pore pressure at "A" (X/L=2.35 & Z'/h=-0.69)

6. APPLICATIONS

Normal wave incidence on an infinitely long composite breakwater over a sand seabed of finite thickness is investigated at a water depth (h) of 28.0cm. The caisson length (bc) is kept as 0.41 of the rubble crown length (b) for all the tested conditions. It is treated as a poro-elastic media with very low porosity of 10% and permeability of 10^{-12}cm/s[7] but rigid with high shear modulus of 10^{12}Dyn/cm^2. The rubble base is 0.3h high over the seabed and has a crown length of 0.425L and side slopes b1/L of 0.08. The permeability of the rubble base and seabed is estimated by Eq.9 as discussed before. The poro-elastic media has a poisson's ratio (v) of 0.33 and a pore fluid bulk modulus (β or BULK) of 10^8Dyn/cm^2 corresponding to 99% pore saturation. **Table 1** summarizes the properties of the waves, breakwater and seabed considered in this work; values in italics refer to the main case study.

Table 1 Calculation conditions for composite breakwater and seabed

Variable	Rubble base	Seabed
H (cm)	*3.0*,4.0	
T (s)	*1.40*,1.80,2.20	
m	0.26,*0.35*,0.45	*0.30*
D (cm)	1,*2*,2.5	*0.10*
ds/L	--	*0.10*,0.17, 0.23,0.30
GS&GF (10^9Dyn/cm^2)	*1.2*,0.12,0.012	*50.0*,5.0,0.5

where ds is the seabed thickness while GS and GF are the shear modulus of the rubble base and seabed, respectively.

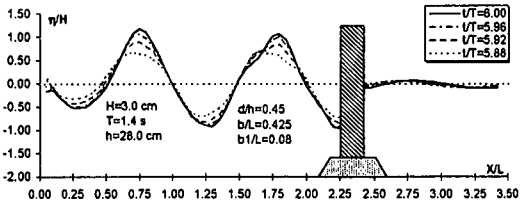

Fig.7 Water levels around the caisson

7. RESULTS AND DISCUSSIONS

(1) Wave-Structure-Seabed Interaction

The instantaneous water levels (η/H) around the caisson are presented in **Fig.7** for H=3.0cm and T=1.4s. Offshore of the caisson, a partial standing wave is formed and has a different profile from the conventional linear one. This is attributed to the nonlinear dynamic interaction with the rubble base. The standing and transmitted waves have heights of 2.40H and 0.17H at the corresponding caisson faces, respectively. The standing wave is greatly influenced by the combined effects of reflection and shoaling over the rubble base.

The transmitted wave has characteristics of a progressive wave with a phase difference from the offshore wave. This phase difference depends on the caisson length and the hydraulic conductivity of the rubble base.

(2) Effect of Hydraulic Properties

The hydraulic properties of the rubble base are mainly represented by the porosity (m) and the mean diameter of the solid particles (D) in the modified Navier-Stokes equations of motion. The effects of D and m on the reflected and transmitted waves are shown in **Figs.8** and **9**. The rubble base absorbs some of the incident wave energy and its hydraulic

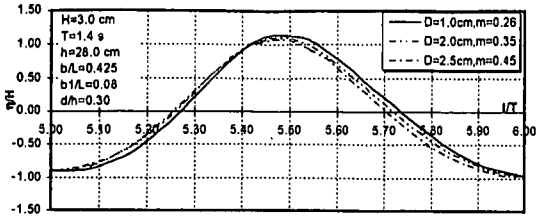

Fig.8 Hydraulic conductivity effect on the offshore wave

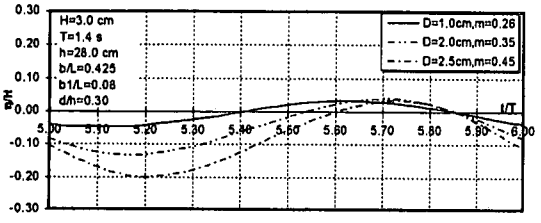

Fig.9 Hydraulic conductivity effect on the onshore wave

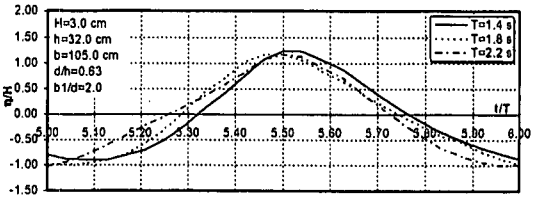

Fig.10 Wave period effect on the offshore wave

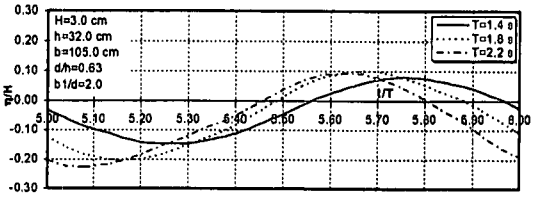

Fig.11 Wave period effect on the onshore wave

conductivity affects the reflected wave (**Fig.8**). The wave height on the offshore face of the caisson decreases from 2.10H (D=1cm and m=0.26) to 2.04H (D=2.5cm and m=0.45) as the rubble base becomes more permeable. As the rubble base becomes less permeable, small D and/or m, the transmitted wave height becomes smaller and its phase difference from the offshore wave varies (**Fig.9**). It can be judged, at least from the examined cases, that the transmitted wave height is sensitive to the hydraulic conductivity of the rubble base since the wave height changes from 0.08H to 0.23H due to its increase. The waves on both faces of the caisson are also observed to have a set-down that increases here as the hydraulic conductivity becomes higher.

(3) Effect of Wave Conditions

To investigate the effect of incident wave conditions, wave periods ranging from 1.4s to 2.2s are tested. However, the breakwater dimensions are kept invariant and similar to that in the hydraulic model experiment. The standing wave height (η/H) on the offshore caisson face generally varies for different wave periods (**Fig.10**); i.e., wave lengths. This is accounted by the fact that the relative size of the protruding part of a rubble base becomes smaller for longer waves and, hence, the shoaling effect over it decreases. The interaction between the waves, main and higher harmonics, reflected from the caisson and the offshore crown corner of the base affects the offshore standing wave along the wave tank. The reduction in shoaling effect is usually dominant for low bases and the standing wave height may approach the theoretical value of 2.0H for a small relative size of the protruding part of a rubble base. The transmitted wave height is found to increase from 0.22H for T=1.4s to 0.32H for T=2.2s. The phase lag from the wave at the offshore caisson face decreases due to the reduction in the relative caisson length, bc/L, and the wave set-down slightly increases (**Fig.11**).

It can be concluded that the size of a caisson and its rubble base compared to the incident wave length has a great influence on the reflected, damped and transmitted waves. Moreover, longer waves have higher capacity to induce waves behind a caisson. This result indicates the need for studying the dynamic interaction between solitary waves of medium height and a composite breakwater to discover their corresponding transmitted waves. Examining the effect of long waves is also recommended when selecting the wave conditions for maximum transmitted wave height behind a caisson.

(4) Structure-Seabed Interaction

The dynamic interaction between a composite breakwater and seabed is evaluated for H=4.0cm, T=1.8s and d/h=0.30. Other dimensions and properties are the same as for the main case study in **Table 1**. The water levels and the pore pressure (Dyn/cm^2) in the porous media are elucidated at t/T=6.0 in **Fig.12**. It has a standing wave height of 2.30H and a transmitted wave height of 0.13H at the offshore and onshore caisson faces, respectively. High pressure gradient in the horizontal direction can be observed under the offshore toe and at the corner of the rubble base causing high dynamic stresses at these locations.

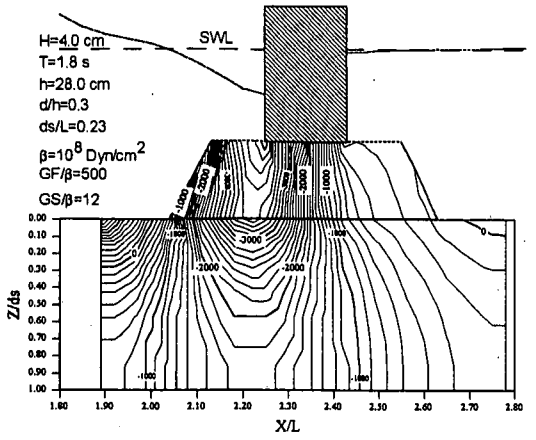

Fig.12 Wave deformation and pore pressure for ds/L=0.23

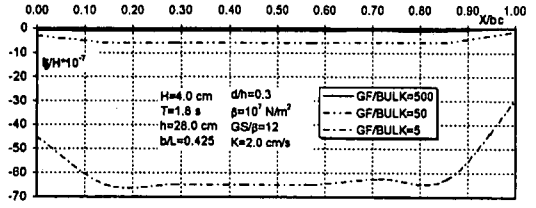

Fig.13 Vertical dsiplacement along the caisson base for GF/β=5~500

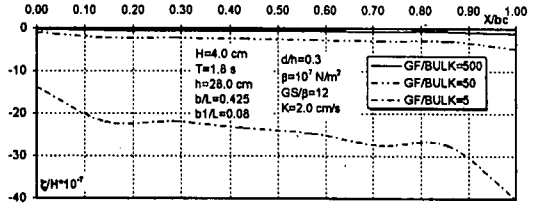

Fig.14 Horizontal displacement along the caisson base for GF/β=5~500

(5) Effect of Seabed Stiffness

The shear modulus of the seabed (GF) affects the solids displacement in the rubble base and the caisson. Therefore, studying the effect of GF on the composite breakwater is crucial toward better understanding of the deformation mechanism of the breakwater and discovering the critical properties of the seabed. The value of GF is changed from 500 to 5 of β and the results are compared and analyzed at t/T=6.0. It is discovered that as GF/β decreases, the vertical and horizontal displacements along the base of the caisson increase (**Figs.13 and 14**). This result may be self explanatory because as the seabed becomes softer, all the solids above it move easier. The pore pressure along the caisson base is found to be almost unchanged here because the spatial distribution of the solids displacement is little influenced by GF. Therefore, the results are not presented here for brevity.

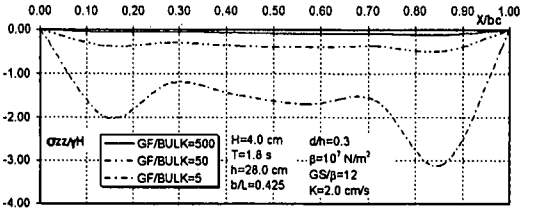

Fig.15 Dynamic vertical stresses along the caisson base for GF/β=5~500

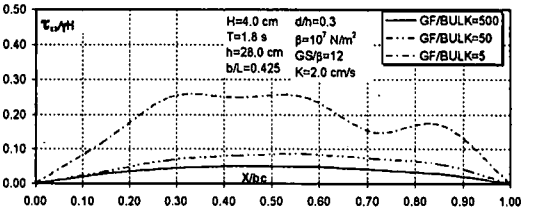

Fig.16 Dynamic shear stresses along the caisson base for GF/β=5~500

The dynamic effective vertical stresses are found to increase significantly along the caisson base, but the increase on the harbor side is more pronounced at this time step (**Fig.15**). The dynamic shear stresses increase significantly such that the distribution pattern deviates from the conventional parabolic one, previously described by Mostafa et al.[12], at a ratio of GF/β=5.0 (**Fig.16**). Also, the peak shear stress moves toward the offshore side as GF/β decreases.

The above results indicate that even if the depth of a soft seabed is small (0.10L), its effect on the dynamic response of a composite breakwater is significant and may endanger its stability under severe wave attack. To have more details on the effect of seabed conditions, the results along the base of the rubble mound are studied for different GF/β and ds/L.

It is found that the solid displacements along the base of the rubble mound generally increases as the shear modulus of the seabed decreases (**Figs.17 and 18**). However, the increase in the vertical displacement is more pronounced than in the horizontal one. This means that the whole composite breakwater has a higher increase in the magnitude of its vertical displacement and more pronounced tendency to move in the zone under the caisson (X/b2=0.35~0.65) over a soft seabed. The pore pressure along the base of the rubble mound is almost unaffected by GF because the pore pressure attenuation inside the rubble is almost unchanged as it has been mentioned earlier. The pore pressure

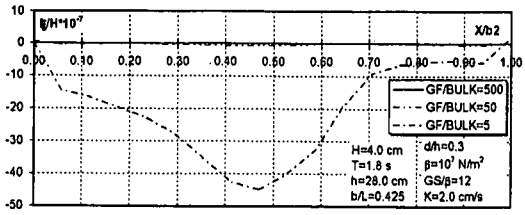

Fig.17 Vertical displacement along the base of the rubble mound for GF/β=5~500

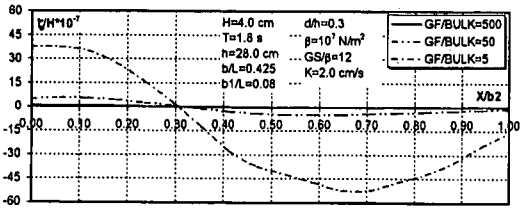

Fig.18 Horizontal displacement along the base of the rubble mound for GF/β=5~500

attenuation inside the seabed is found to be affected by GF (**Fig.19**). The softer the seabed, the higher the attenuation of pore pressure in the seabed for GF/β>5. The effect of GF may not be very pronounced in this case since the seabed thickness is small compared with the wave length (ds/L=0.10), but it is expected to be more pronounced for a larger seabed thickness (ds).

The dynamic vertical stresses are found to decrease on the offshore side and slightly increase on the harbor side as GF/β changes from 500 to 50 (**Fig.20**). But if GF/β changes from 50 to 5, it is remarked that the distribution pattern of vertical stresses changes its shape on the offshore side, but the values only increase on the onshore side. Moreover, the vertical stresses in the zone under the caisson change from compression to tension and the point of maximum vertical stress is shifted to the zone under the center of the caisson. Comparing the magnitude of vertical stresses along the base of the caisson (**Fig.15**) and over the seabed (**Fig.20**), it can be realized that the rubble base plays a key role in reducing the stresses over a soft seabed. It is also noticed that, in case of soft seabed, the dynamic vertical stresses are concentrated under the caisson even with the use of the rubble base. However, in case of hard seabed, they are distributed over a wider area along the base of the rubble mound. The dynamic shear stresses along the base of the rubble show similar changes to that in case of the vertical stresses, but the maximum shear stresses occur under the edges of the caisson as GF/β decreases from 50 to 5 (**Fig.21**).

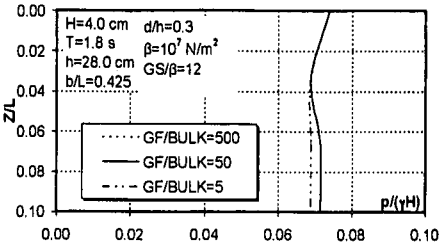

Fig.19 Pore pressure magnitude under the onshore toe of a rubble base for GF/β=5~500

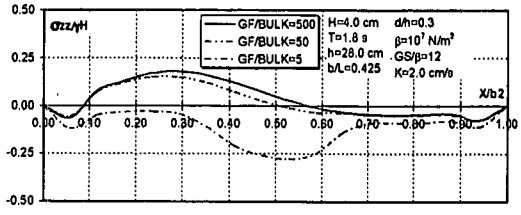

Fig.20 Dynamic vertical stresses along the base of the rubble mound for GF/β=5~500

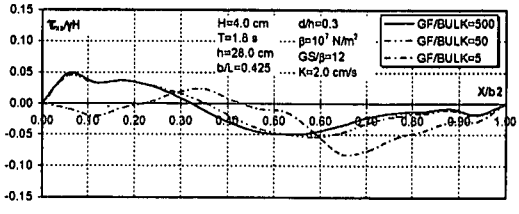

Fig.21 Dynamic shear stresses along the base of the rubble mound for GF/β=5~500

(6) Effect of Rubble Base Stiffness

By changing the stiffness ratio (GS/β) of the rubble mound from 12 to 0.12, it becomes evident that GS/β affects the solids displacement and dynamic stresses along the base of the caisson at t/T=6.0. The less GS/β is, the larger the vertical and horizontal solid displacements are along the base of the caisson, but keeping the distribution pattern almost unchanged (**Figs.22** and **23**). However, the dynamic effective vertical and shear stresses along the caisson base slightly decrease as GS/β decreases (**Figs.24** and **25**). This may occur because the stresses are function of both the shear modulus and the spatial variation of the solid displacement. Reducing the shear modulus normally increases the displacements and affects their distribution but this may be at a less rate than the decrease in the shear modulus. Therefore, smaller values of the shear modulus increase the displacement but may decrease the stresses along the caisson base.

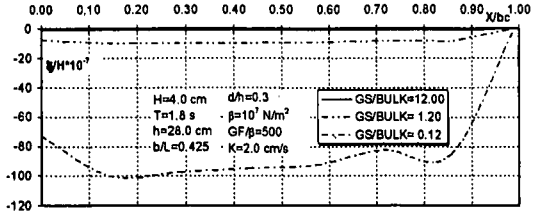

Fig.22 Vertical displacement along the caisson base for GS/β=0.12~12.0

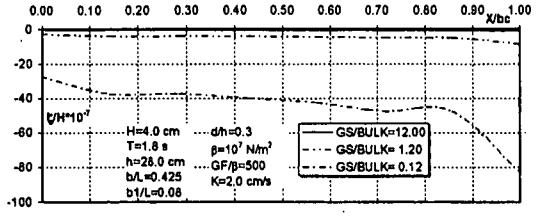

Fig.23 Horizontal displacement along the caisson base for GS/β=0.12~12.0

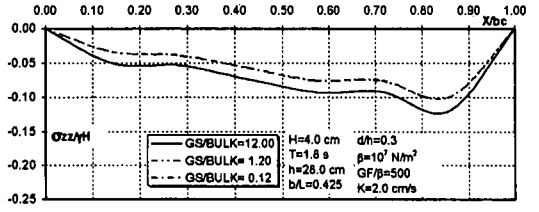

Fig.24 Dynamic vertical stresses along the caisson base for GS/β=0.12~12.0

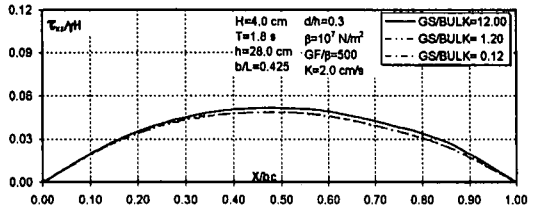

Fig.25 Dynamic shear stresses along the caisson base for GS/β=0.12~12.0

It is detected that the effect of the shear modulus of the rubble base on the pore pressure along the bases of the caisson and rubble mound is negligible for GS/β>1. In this study, the pressure distribution along the base of the caisson is affected slightly by the shear modulus of the rubble at GS/β=0.12 but is not affected for GS/β>0.12. Moreover, the reduction in GS/β increases slightly the vertical displacement along the base of the rubble only in the zone under the caisson and offshore from it (**Fig.26**). The horizontal displacement and dynamic stresses along the base of the rubble mound are almost unaffected by GS/β in this case. This may be due to the high stiffness (GF/β) and small thickness of the seabed under the composite breakwater.

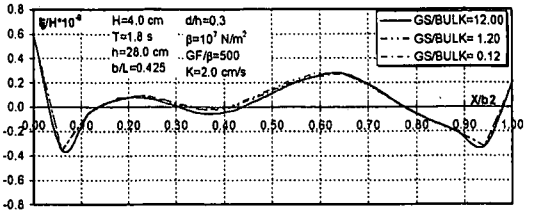

Fig.26 Vertical displacement along the base of the rubble mound for GS/β=0.12~12.0

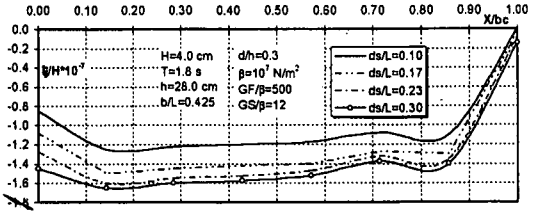

Fig.27 Vertical displacement along the caisson base for ds/L=0.10~0.30

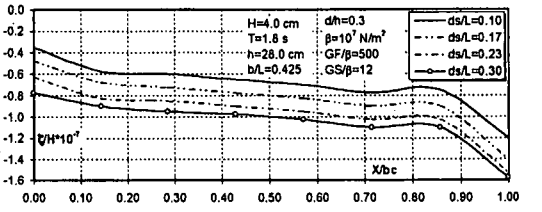

Fig.28 Horizontal displacement along the caisson base for ds/L=0.10~0.30

(7) Effect of Seabed Thickness

The dynamic interaction between a composite breakwater and its seabed foundation is investigated for ds/L=0.10~0.30 and the results are also compared at t/T=6.0. It is found that the vertical and horizontal solid displacements along the base of the caisson increase as the thickness of the seabed increases without changing their distribution pattern (**Figs.27** and **28**). The pore pressure along the caisson base may change slightly due to the increase in the seabed thickness (**Fig.29**). This may be accounted by the increase in caisson displacement. The dynamic vertical stresses along the base of the caisson are found to increase slightly under the harbor edge of the caisson and decrease under its offshore edge due to increasing ds/L (**Fig.30**). The shear stresses are almost unaffected by ds/L so, for brevity, the results are not presented here. This is accounted by the fact that the dynamic shear stresses depend on the spatial variation in the displacement rather than its magnitude. Since the spatial variation of the displacement does not change, it makes sense that the dynamic shear stresses remain unchanged.

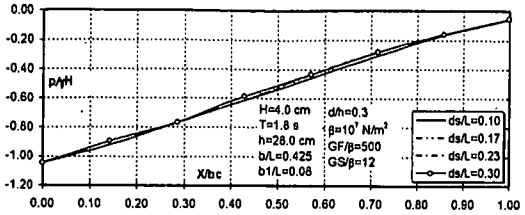

Fig.29 Pore pressure along the caisson base for ds/L=0.10~0.30

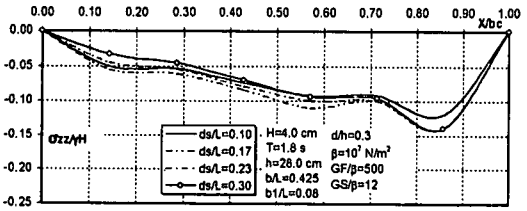

Fig.30 Dynamic vertical stresses along the caisson base for ds/L=0.10~0.30

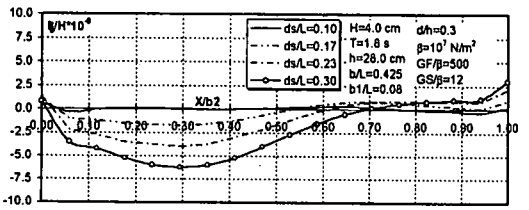

Fig.31 Vertical displacement along the base of the rubble mound for ds/L=0.10~0.30

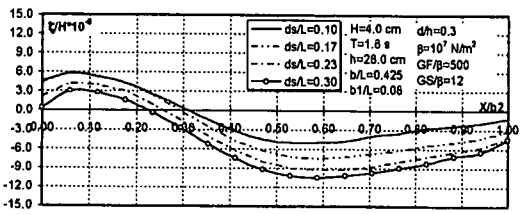

Fig.32 Horizontal displacement along the base of the rubble mound for ds/L=0.10~0.30

The vertical and horizontal solid displacement along the base of the rubble are found to increase for larger ds/L without significant effect on their spatial variation (**Figs.31** and **32**). The displacement values are also damped from the base of the caisson to that of the rubble mound. The pore pressure along the base of the rubble changes slightly in the zone under the caisson, but there is almost no change away from this zone (**Fig.33**). It may be thought that the change in the caisson displacement and pore flow, due to the change in ds/L, affects the pore pressure under the caisson.

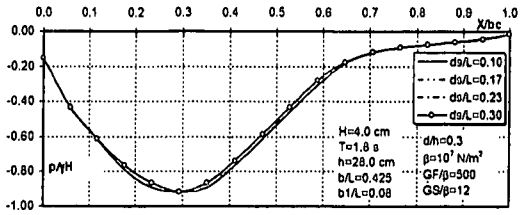

Fig.33 Pore pressure along the base of the rubble mound for ds/L=0.10~0.30

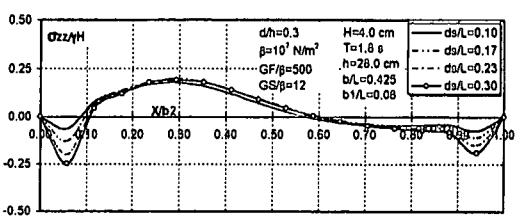

Fig.34 Dynamic vertical stresses along the base of the rubble mound for ds/L=0.10~0.30

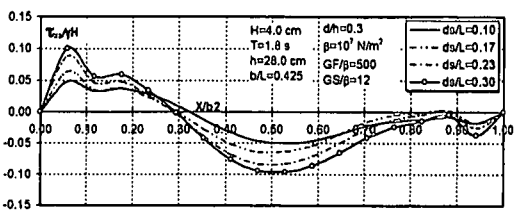

Fig.35 Dynamic shear stresses along the base of the rubble mound for ds/L=0.10~0.30

The dynamic vertical stresses along the base of the rubble mound increase slightly in the zone under the caisson but increase appreciably under both ends of the rubble base as ds/L increases (**Fig.34**). This indicates that there is a great possibility of toe failure due to liquefaction/slip failure under severe wave attack in case of constructing the breakwater over a sand seabed of large thickness. It can be judged from these results that the dynamic vertical stresses in the area under the caisson become independent of the seabed thickness for ds/L>0.17. The dynamic shear stresses also increase as ds/L increases but keeping the distribution pattern unchanged (**Fig.35**). A significant increase in the stresses is observed under the offshore toe of the rubble base.

(8) Pore Pressure at the Offshore Toe

The instantaneous pore pressure attenuation in the seabed under the offshore toe of the rubble base increases for large ds/L (**Fig.36**). This location is far from the effect of the caisson displacement and, hence, it is more likely that the change in the pore

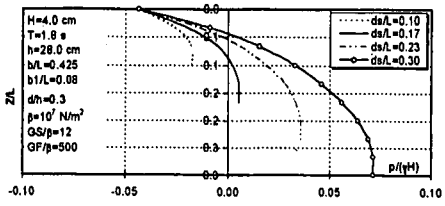

Fig.36 Pore pressure under the offshore toe of a rubble mound base at t/T=5.75

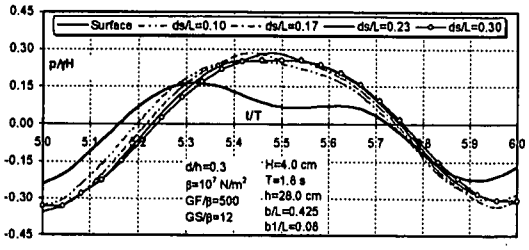

Fig.37 Pore pressure under the offshore toe of a rubble mound base at Z/L=0.10

pressure is due to the change in the propagation of the nonlinear wave harmonics in the seabed rather than the caisson displacement. The nonlinear wave harmonics, inside the seabed, exhibit a different phase delay that depends on wave period and varies due to the change of ds/L. In this study, the harmonics seem to interact constructively due to the change in their phase difference and, hence, the magnitude of pore pressure in the seabed at some points becomes higher than its magnitude at the seabed level (**Fig.37**). Thus, a large excess pore pressure may be developed at this location. This phenomena seems to depend on the location of the toe in the wave field, existence of higher harmonics and properties of the porous media as well as the seabed thickness. Analysis of this phenomena deems necessary.

It should be kept in mind that the wave harmonics have a 2-D propagation in the poro-elastic media and the zone under the toe is influenced by the interaction between the pore pressure passing through the rubble base to the seabed and the wave-induced pressure by the offshore wave at the seabed level (Pb). Therefore, it is found that the pore pressure under the offshore toe becomes less than the surface pressure if the permeability of the rubble base is small enough to damp the pore pressure allowing a small part passing to the seabed (**Fig.38**). This suggests that a zone under the rubble base of a composite breakwater exists in which the use of a 1-D equation to evaluate the pore pressure should be avoided.

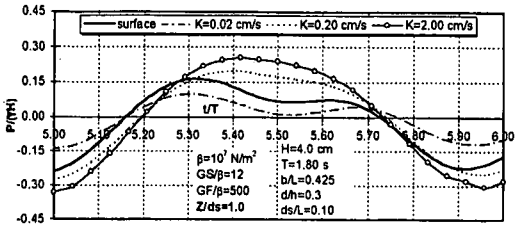

Fig.38 Effect of rubble base permeability on pore pressure under its offshore toe

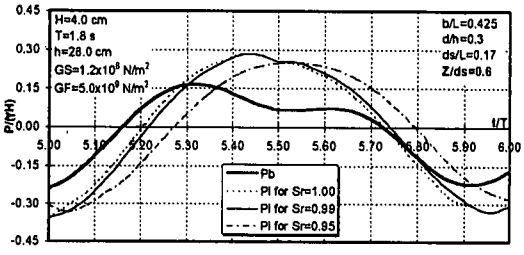

Fig.39 Effect of pore fluid compressibility on pore pressure under the offshore toe of a rubble base

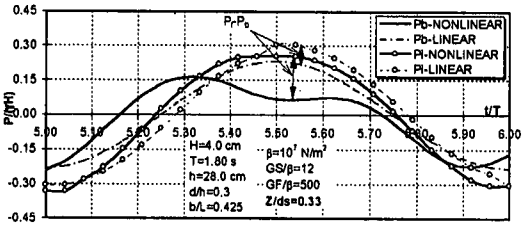

Fig.40 Effect of nonlinear boundary pressure on pore pressure under the offshore toe of a rubble base

The compressibility of pore fluid may cause a phase delay in the pore pressure in the seabed (Pi) that depends on wave period[20] and, hence, the interaction between nonlinear wave harmonics under the offshore toe varies consequently as shown in **Fig.39**.

To show the influence of using the nonlinear boundary pressure, the boundary pressure for linear standing waves[7] is employed and the pore pressure results are compared with the previous results (**Fig.40**). It is clear that the interaction between the pressure passing from the rubble base to the seabed and that due to the wave at the offshore is still evident for linear boundary pressure, however, the excess pore pressure (P_i-P_b) is much less than the case of nonlinear boundary pressure.

The wave conditions and the location of the toe in the wave field influence the occurrence of such phenomena as well. The pore pressure under the offshore toe of a composite breakwater is analyzed for two wave heights, H=3.0cm and 5.0cm, and

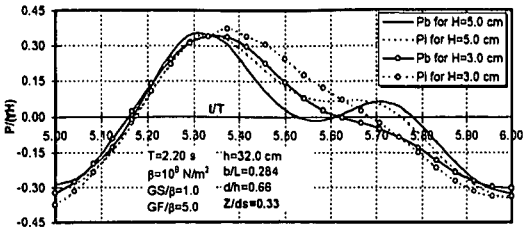

Fig.41 Effect of wave nonlinearity on the pore pressure at the offshore toe of a rubble base

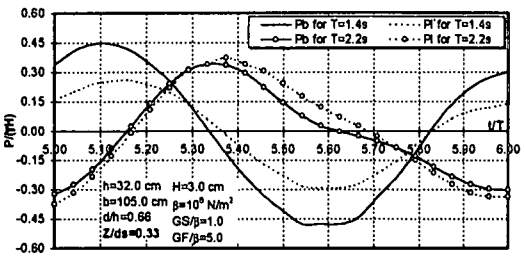

Fig.42 Effect of toe location in the wave field on excess pore pressure under it

T=2.2s (**Fig.41**). The dimensions of the breakwater and seabed are the same as the hydrulic model. The porewater is considered to have less than 0.01% air content to exclude the effect of pore fluid compressibility. The development of a secondary crest is more evident for H=5.0cm and the excess pore pressure becomes more appreciable than for H=3.0cm. This elucidates the contribution of wave nonlinearity (H/h) to the occurrence of a large excess pore pressure at the offshore toe.

The influence of toe location in the wave field is examined through comparing the results for H=3.0cm while the offshore toe is at X/L=1.83 and 2.07 for T=1.4s and 2.2s, respectively. The pore pressure magnitude in the seabed is less than the pressure at the mud line while the excess pore pressure is larger at t/T≅5.6 for X/L=1.83 compared with the case of X/L=2.07 (**Fig.42**). However, the maximum excess pressure occurs during the phase of negative pressure at the mud line similar to the case of progressive waves for X/L=1.83, but it may happen during the phase of positive pressure at the mud line for X/L=2.07. It is noteworthy that the offshore toe of the composite breakwater is at X/L=2.045 for the main case study. It may be thought that when the pressure acting on the rubble base slope is larger than that at the offshore toe, the pressure passing the rubble base to the seabed may enhance the magnitude of pressure in the seabed. This may cause the pressure magnitude in the seabed to be larger than that at the mud line.

8. CONCLUSIONS

1. The hydraulic conductivity of a rubble mound base has a significant effect on the nonlinear standing wave when the size of its protruding part is comparable to the water depth and/or the wave length. The transmitted wave to the leeward of the breakwater has a phase lag that depends on the relative length of the caisson (bc/L) and hydraulic conductivity of the rubble base. The transmitted wave height increases as the rubble base hydraulic conductivity increases or its relative size and bc/L decrease. Thus, long waves have higher capacity to induce waves on the harbor side than shorter ones. The effect of the transmitted wave on the stability of the breakwater depends on its phase difference from the standing wave on the offshore side.

2. The pore pressure along the base of the caisson is found to be slightly affected by the shear modulus of the rubble base (GS) for GS/β<1 in case of a hard sand seabed. This effect is anticipated to be more pronounced for a soft seabed. The pore pressure along the base of the rubble mound and the caisson is found to be almost unaffected by the shear modulus of the seabed (GF) for small values of the seabed thickness (ds/L), but it is influenced in the seabed. The pore pressure along the base of the caisson and the rubble mound is little affected by the seabed thickness.

3. The spatial distribution of the dynamic shear stresses along the base of the caisson and rubble mound is affected by the shear modulus of the seabed. The assumption that the stresses under the base of the caisson are transmitted to the seabed at a certain slope does not work well in case of wave loading and considering the wave-induced flow and solids displacement in the rubble base. This assumption neglects the wave-induced stresses in the rubble base and the hydraulic and geotechnical properties of the rubble base and seabed. For a seabed of large thickness, high dynamic vertical and shear stresses are found to occur under the ends of the rubble base threatening its stability.

4. The rubble base is found to play a key role in damping the solid displacement and redistributing the dynamic stresses over a soft sand seabed. The dynamic interaction between a composite breakwater and its seabed foundation is revealed to depend greatly on the seabed stiffness and thickness.

5. The development of a pore pressure in the seabed under the offshore toe larger than that at the mud line over it depends on the hydraulic conductivity of the rubble base and location of the offshore toe. This causes a large excess pore pressure that varies according to the seabed thickness, pore fluid compressibility and wave nonlineariy. The use of a boundary pressure for linear waves and ignoring the rubble base effect on the wave field shows the same phenomena but with large differences in magnitude and phase. The seabed zone offshore of the rubble base is vulnerable to liquefaction especially where the nonlinear wave harmonics interact in the seabed constructively. This becomes more likely if the node is close to the offshore toe in a highly nonlinear wave field.

ACKNOWLEDGEMENT: The second author is on leave from the Department of Irrigation and Hydraulics in the Faculty of Engineering of Cairo University, Giza, Egypt.

REFERENCES

1) Oumeraci, H.: Review and analysis of vertical breakwater failures-lessons learned, *Coastal Eng.*, Elsevier, Vol. 22, pp. 3-29, 1994.
2) Oumeraci, H. and Kortenhaus, A.: Analysis of the dynamic response of caisson breakwater, *Coastal Eng.*, Elsevier, Vol. 22, pp. 159-183, 1994.
3) Kortenhaus, A. , Oumeraci, H., Kohlhase, S. and Klammer, P.: Wave-induced uplift loading of caisson breakwaters, *24th ICCE*, ASCE, pp.1298-1311, 1994.
4) Sulisz, W.: Numerical modelling of the stability of rubble bases, *23rd ICCE*, ASCE, pp.1799-1809, 1992.
5) McDougal, W.G, Tsai, Yau-Tang and Sollitt, C.K.: Verification of the analytical model for ocean wave-soil-caisson interaction, *20th ICCE*, ASCE, pp.2089-2103, 1986.
6) Tsai, Yau-Tang, McDougal, W.G. and Sollitt, C.K.: An analytical model for ocean wave-soil-caisson interaction, *20th ICCE*, ASCE, pp.2314 -2328, 1986.
7) Mase, H., Sakai, T. and Sakamoto, M.: Wave-induced pore-water pressures and effective stresses around breakwater, *Ocean Eng.*, Elsevier, Vol.21, No.4, pp. 361-379, 1994.
8) Mizutani, N., McDougal, W. and Mostafa, A.: BEM-FEM combined analysis of non-linear interaction between wave and submerged breakwater, *25th ICCE*, ASCE, pp.2377-2390, 1996.
9) McCorquodale, J.A., Hannoura, A.A. and Nasser, M.S.: Hydraulic conductivity of rockfill, *J. Hydraulic Research*, Vol.2, pp. 123-137, 1978.
10) Mostafa, A. and Mizutani, N.: Numerical analysis of dynamic interaction between non-linear wave and impermeable seawall with permeable rubble toe resting over a sand seabed, *ISOPE 97*, Vol. 3, pp.823-830, 1997.
11) Mizutani, N., Mostafa, A. and Iwata, K.: Non-linear regular waves, submerged breakwater and seabed dynamic interaction, *Coastal Eng.*, Elsevier, Vol.33, pp.177-202, 1998.
12) Mostafa, A., Mizutani, N. and Iwata, K.: Non-linear wave, composite breakwater and seabed dynamic interaction, *J. of Waterway, Port, Coastal and Ocean*, ASCE, Vol.125, No.2, 1999.
13) Ohyama, T. and Nadaoka, K.: Development of a numerical wave tank for analysis of non-linear and irregular wave field, *Fluid Dynamics Research*, Vol.8, pp. 231-251, 1991.
14) Brorsen, M. and Larsen, J.: Source generation of non-linear gravity waves with the boundary integral equation method, *Coastal Eng.*, Elsevier, Vol.11, pp. 93-113, 1987.
15) Biot, M.A.: General theory of three-dimensional consolidation, *J. appl. Phys.*, Vol.12, pp. 155-164, 1941.
16) Ergun, S.: Fluid flow through packed columns, *Chem. Eng. Prog.*, Vol. 48(2), pp.89-94, 1952.
17) Dudgeon, C.R.: An experimental study of the flow of water through coarse granular media, *La Houille Blanche*, Vol.7, pp.785-801, 1966.
18) Yamamoto, T., Koning, H.L., Sellmeijer, H. and Hijum, E.V.: On the response of a poro-elastic bed to water waves, *J. Fluid Mech.*, Vol.87, pp.193-206, 1978.
19) Mizutani, N. and Mostafa, A.: A study on dynamic response of foundation of composite-type breakwater to non-linear waves, *Proc. of Coastal Eng.*, JSCE, Vol.44, pp.926-930, 1997.
20) Mizutani, N. and Mostafa, A.: Nonlinear wave-induced seabed instability around coastal structures, *Coastal Eng. Journal*, JSCE, Vol.40, No.2, pp.131-160,1998.

(Received January 26, 1998)

砂層上の混成堤と波の非線形相互作用に関する数値解析

水谷法美・ Ayman M. MOSTAFA ・岩田好一朗

著者らが開発したBEM-FEM解析モデルとPoro-Elastic FEM解析モデルを，波・混成堤・海底地盤の相互干渉が解析できるように改良するとともに，水理模型実験を行ってそれらの妥当性を検証した．Poro-Elastic FEM 解析モデルには，新たに非線形ダルシー則に基づいて評価した透水係数を採用したので，その精度は向上した．本解析手法は，波動場のみならず間隙水圧も精度良く計算できることを明らかにした．さらに混成堤マウンド先端部では，間隙水圧の勾配が大きく，液状化などの発生の可能性が高くなることを明らかにした．